Sprayable Antibacterial Film:

A Nanosilver Composite

Nathan Cloeter, Luis Correa, Benjamin Lee, Matt Reilly, Mercedes Valero

Recent studies suggest that cell phones are one of the surfaces with the most bacteria we encounter in our day, where it was shown that 1 in 6 cellphones are contaminated with fecal matter (Song). Silver nanoparticles have been shown to be highly efficient antibacterial nanoparticles, largely due to the oxidation and release of silver ions (Ferrer, Guo). Composite materials with antibacterial polymers and silver nanoparticles expand the applications of silver nanoparticles for antibacterial purposes, especially because they can be used as coatings for a variety of applications. These composites are beneficial because the nanoparticles can prevent bacterial growth while the polymer can prevent bacterial adhesion. This design takes advantage of the inherent antibacterial properties of chitosan, a polysaccharide extracted from shrimp shells, and the silver nanoparticles to produce a chitosan based polymeric coating with enhanced antibacterial properties. In the design, the properties of the sprayable solution, the nanoparticle formation kinetics and the film properties were studied. We also report on the results from the preliminary prototyping and antibacterial testing of films designed to be applied to the Aluminum back of the iPhone 5.

TABLE OF CONTENTS

1. MOTIVATION

Advances in biotechnology have opened opportunities for novel uses of materials in the medical field. Because of the tailorability, high surface area, homogenous particle distribution and simple synthesis of nanoparticles, they pose the opportunity for the greatest advances in medicine. One such opportunity is the development of antibacterial films. These films have applications in internal medical devices such as wound coverings, and even food processing containers (Moritz). Silver nanoparticles have been shown to be highly efficient antibacterial nanoparticles, largely due to the oxidation and release of silver ions (Ferrer, Guo). Composite materials with bactericidal polymers and silver nanoparticles expand the applications of silver nanoparticles for antibacterial purposes, especially because they can be used as coatings for a variety of applications. These composites are beneficial because the nanoparticles can prevent bacterial growth while the polymer can prevent bacterial adhesion. These are known as release-killing and capture-killing mechanisms, respectively. This would open the applications beyond the antibacterial capabilities of nanoparticles and into applications where capture-killing and release-killing properties work to provide materials with higher antibacterial properties.

It has been recognized that silver nanoparticles have a limited lifetime of bactericidal activity. This led our team to believe that a sprayable coating would be exceedingly beneficial to the field. Having the ability to selectively make a surface antibacterial not only allows for versatility, but also compensates for the degradation of antibacterial activity, as it can be reapplied as needed. Developing a novel composite with such a composition would further the applications and possibilities of antibacterial coatings and films. Furthermore, little research has been done with regards to sprayable antibacterial films, where the majority is concentrated around wound coatings and medical purposes. We saw the opportunity to develop a commercial product, which would be challenging and exciting for a senior design project.

2. UPDATED PROPOSED WORK & PERFORMANCE

Our project focused on designing a sprayable thin antibacterial film to be used on the back of the Apple iPhone 5. Furthermore, our design allows for a versatility in applications if it were to be further developed. The design consisted of a film that can be sprayed onto the anodized aluminum surface of the iPhone 5, dry to a thickness of 50 µm within 8 hours, adheres to the aluminum oxide layer in order to be durable for at least 2 months, and provides antibacterial properties that provide a maximum colony-forming unit (CFU) of 5×10^5 per mL of film solution. A feasible antibacterial property for the film was determined based on previous experimentations, as the full antibacterial nature of silver

nanoparticles is not fully elucidated (Reigel). The thickness of the film is based on the typical cell phone screen protection films, the 8 hours drying time would allow the used to spray the phone before going to sleep to wake up with a coated phone, and the additional design goals are based on what we believe to be consumer needs and previous research which sets expectable limitations on our design.

A composite solution was designed and prototypes were made with the appropriate composition of chitosan, levan and silver nanoparticles to achieve a sprayable viscosity, while still maintaining antibacterial properties comparable to previous research in composite films. The design also included polyethylene glycol (PEG), however, it was not included into the prototype due to time constraints. The solution was designed to suspend silver nanoparticles within a chitosan matrix, as shown by Wei et.al, where the nanoparticles are synthesized *in situ* within the chitosan. The chitosan stabilizes the nanoparticles, preventing agglomeration and limiting ion release, in addition to having antibacterial properties. Additionally, levan was included in the design to improve adhesive and mechanical properties of the film. Levan is a sugar-derived polysaccharide that also possesses antibacterial properties similar to chitosan; and like chitosan, levan resists bacterial adhesion (Esawy). Lastly, PEG was included in the design to increase the water retention and permeability of the polymer matrix, ensuring an adequate environment for silver ion diffusion. Also, as a plasticizer, PEG will also alleviate the brittleness levan confers to the film.

3. TECHNICAL APPROACH

3.1 SOLUTION PROPERTIES

3.1.1 SOLUBILITY OF CHITOSAN
Chitosan is soluble in weak acids, and most commonly dissolved in 1% acetic acid. The viscosity of the solution was set to a range between 100-200 cp, comparable to many olive oils and maple syrup, where the ideal viscosity is near 180 cp (described in section 3.1.2). We found that 10 mg of chitosan dissolved in 20 ml of 1% acetic acid produce the solution with the 100-200 cp viscosity range. While we understand that given enough pressure most fluids can be sprayed, this is a design for a finger pump, so the fluid must be sprayed with minimal effort.

3.1.2 SOLUTION NEEDS AND VISCOSITY
Primarily, our solution needs to have a sprayable viscosity. Lower viscosities will increase sprayability and decrease droplet size, providing a thinner and more even film upon application. Viscosity is also

useful to determine the mobility of the silver nanoparticles in the solution. Slower particle settling will occur in a more viscous solution. In order to determine an ideal viscosity for our design we developed the following equation:

$$\mu_{solution} = 0.8\mu_{spray} + 0.2\mu_{settle}$$

This serves as a weighted system by which to determine the viscosity accounting for our needs. μ_{spray} is the researched viscosity for optimal sprayability of a polymeric solutions, 200 cp, and μ_{settle} is the calculated viscosity for the optimal settling under drying conditions, 113 cp, the calculations which can be found in section 3.1.4. Because the addition of chitosan to our solution both increases antibacterial efficacy, as chitosan is intrinsically antibacterial, and increases the solution viscosity, due to polymerization, our design proceeds with the assumption that higher concentrations of chitosan are better. These calculations render an ideal viscosity of 182.72 cp.

3.1.3 VISCOSITY MEASUREMENT TECHNIQUE

Viscosity measurements were taken with a Brookfield viscometer, model DV-E. Access to the equipment was provided by the University of Maryland Energy Research Center in Dr. Eric Wachsman's laboratory. The instrument is frequently used by the graduate students working in the laboratory and has been calibrated with fluids provided by the manufacturer in the past.

3.1.4 NANOPARTICLE SETTLING

The setting of the nanoparticles is both important to the solution before it is sprayed and while it is drying into the film. The distribution of the nanoparticles is important to have uniform antibacterial properties throughout the film. Because a solution in a bottle can be shaken or stirred, the settling of nanoparticles during film drying is more important than the settling in solution.

Settling in this case in determined by Stoke's law, on account of the laminar flow of the solution and the small particle size. Stoke's law on drag, states that

$$F = 3\pi\mu Vd$$

where *F* is the force of drag, the fluid viscosity is *μ*, which equals μ_{settle} described in section 3.1.4, *d* is the diameter of the sphere and *V* is the velocity of the sphere. By equating the viscous drag to the effective gravitational force we can obtain the terminal falling velocity, or settling velocity.

$$3\pi\mu V_0 d = \frac{\pi d^3}{6}(\rho_p - \rho_f)g$$

6

$$V_0 = \frac{D^2(\rho_p - \rho_f)g}{18\mu}$$

where V_0 is the settling rate, ρ_p and ρ_f are the densities of the particle and fluid, respectively (Richardson). That equation can be rearranged to give an ideal viscosity based on a maximum settling velocity.

$$\mu_{settle} = \frac{D^2(\rho_p - \rho_f)g}{18 \bullet V_{settle}}$$

Analyzing the spray application of the film will allow us to determine the thickness of the sprayed solution and a viable settling rate that does not hinder antibacterial properties. In order to best test our film production, we approached the film fabrication by adding 10ml of solution to a 10cm radius petri dish. This results in a 'wet' thickness of approximately 63µm. Given our design goal of achieving a 50µm thick film, this would indicate that there is a film reduction of 13µm over 8 hours, or 1.625µm/hr. Using that as our V_{settle} parameter, and a conservative particle size of 100nm, we calculate a viscosity of 113.6 cp for ideal settling.

3.1.5 SOLUTION KINETICS

We investigated the nanoparticle kinetics in the chitosan solution and matrix. The Gibbs-Thomson effect, frequently used to determined phase equilibrium and phase transformations, describes the effect of surface energy on particle size, and is given by

$$\Delta G_\gamma = \frac{2\gamma Vm}{r}$$

where ΔG_γ is the Gibbs free energy of the particle, γ is the surface energy, V_m is the volume of particle and r is the radius of the particle. Although the Gibbs-Thomson equation supposes equilibrium, which we do not assume to have within our system, the Gibbs-Thomson effect can also be used to determine the amount of energy required to create a particle of a certain radius, as shown below

$$\Delta G = \frac{4}{3}\pi r^3 \Delta G_v + 4\pi r^2 \gamma$$

where ΔG_v is the Gibbs free energy per volume. This relationship shows that larger radii particles require greater energies of formation. The free energy per volume can be described with the following equation (Pierre)

$$\Delta G_v = \frac{-k_b T}{\ln(C/C_0)}$$

where k_b is the Boltzmann constant, T is temperature, C is the solute concentration and C_0 is the equilibrium concentration. The relationship between a nucleating particle size and free energy can further be explained with Figure 1 below, showing that there is a critical radius at a critical change in the Gibbs energy. Below this radius, nuclei will not form. The solid will begin to nucleate according to the balance between the interfacial and volumetric free energies.
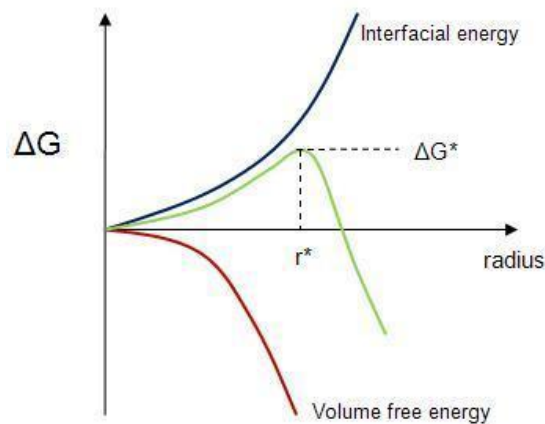

Figure 1: *Critical radius for nuclei formation.* (Wikipedia Commons images)

The previous equations for the Gibbs-Thompson effect shows us that both the critical free energy and radius size depend on the free energy per volume as follows

$$\Delta G^* = \frac{16\pi\gamma}{3(\Delta G_v)^2}$$

$$r^* = \frac{-2\gamma}{\Delta G_v}$$

by substituting in our equation for ΔG_v we can derive the following expression that relates the critical radius with concentration and temperature

$$r^* = \frac{2\gamma \ln(C/C_0)}{k_b T}$$

which tells us that smaller solute concentrations, which are effectively ionic concentrations, could result in smaller radii, and smaller radii can also be achieved with increasing temperature.

3.1.6 YOUNG-DUPRE EQUATION

Young-Dupre equation is important in this design because it can be used to determine the solution's wettability on a substrate, as well as, to determine adhesion properties of the film on the substrate. Wetting is the ability of the solution to maintain contact with the substrate's surface. This is a result of intermolecular interactions between the solid, liquid and gas phases. The interactions between the solid and liquid phases are closely related to the material's adhesive properties, where high adhesive interactions lead to low contact angles between the liquid and the solid substrate, which implies high wettability. The Young's relation responsible for the determination of surface wetting is given by

$$\gamma_{SG} = \gamma_{SL} + \gamma_{LG}\cos\theta$$

where γ_{SG} is the surface tension between solid and gas, γ_{SL} is the surface tension between solid and liquid, γ_{LG} is the surface tension between liquid and gas and θ is the contact angle between the solid liquid interface. While we know the surface energy of aluminum oxide to be between 31 mN/m and 50 mN/m, depending on how it is cleaned. However, determining the surface energy of the solution would require intense analysis of the wetting angle of our solution on the substrate. The surface energy of aluminum oxide is high compared to many polymeric materials, but low compared to various ceramics such as glass. Because the surface energies between the liquid and the substrate and the liquid and the gas are difficult to approximate based on solution properties, we proceed with our design assuming that the medium surface energy of aluminum oxide would result in appropriate wetting.

A second form of the Young-Dupre equation useful in this design relates the amount of work required to cleave bonded interfaces, creating new surfaces, sometimes referred as "work of adhesion". For two equal surfaces, the work required to create two new surfaces is given by

$$W = 2\gamma$$

where γ is the surface energy of each new surface. In this design, two distinct surfaces are created when the film is pulled off the substrate. In this case, the work of adhesion is given by
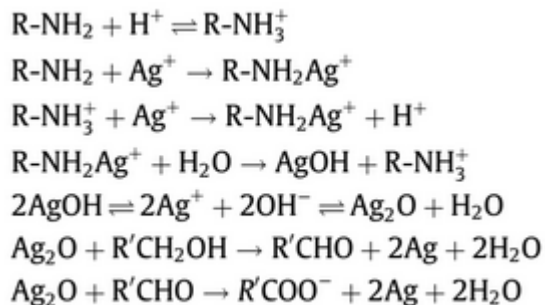
$$W_{12} = \gamma_1 + \gamma_2 - \gamma_{12},$$

where γ_1 and γ_2 are the surface energies of the two new surfaces, and γ_{12} is the interfacial tension. We also considered other types of adhesion mechanisms between the film and substrates, which are reported below.

3.2 NANOPARTICLE PROPERTIES

3.2.1 FORMATION/SYNTHESIS OF NANOPARTICLES

The process for the formation of silver nanoparticles in chitosan was followed by the procedure that was published by Wei. The nanoparticles were synthesized by mixing silver nitrate into a chitosan solution. The acetylation of the chitosan, which is effectively deacetylated chitin, is the driving force behind the reduction of the silver ions (Wei 2). Below is the pathway silver undergoes to precipitate in solution (Wei 2).

$$R\text{-}NH_2 + H^+ \rightleftharpoons R\text{-}NH_3^+$$
$$R\text{-}NH_2 + Ag^+ \rightarrow R\text{-}NH_2Ag^+$$
$$R\text{-}NH_3^+ + Ag^+ \rightarrow R\text{-}NH_2Ag^+ + H^+$$
$$R\text{-}NH_2Ag^+ + H_2O \rightarrow AgOH + R\text{-}NH_3^+$$
$$2AgOH \rightleftharpoons 2Ag^+ + 2OH^- \rightleftharpoons Ag_2O + H_2O$$
$$Ag_2O + R'CH_2OH \rightarrow R'CHO + 2Ag + 2H_2O$$
$$Ag_2O + R'CHO \rightarrow R'COO^- + 2Ag + 2H_2O$$

This mixture was stirred and heated for 12-14 hours depending on laboratory availability. We found this reaction proceeds at room temperature, and that the addition of heat serves to accelerate the rate of silver nucleation. In section 3.1.5 it is shown that the critical radius for nucleation can be influenced with solute concentration as well as temperature. A yellow-orange coloring can indicate the presence of nanoparticles in the solution.

3.2.2. ANTIBACTERIAL NATURE OF SILVER NANOPARTICLES

The antibacterial activity of silver has only recently been elucidated by a few proposed theories. One theory proposes the formation of sulfide linkages between thiol groups in the cell membrane and the silver atoms, which lead to a consequent change in the shape and function of affected proteins and the disruption of cell integrity (Klueh). Another theory proposes that silver ions enter the cell and denatures

its DNA through intercalation with nucleic acids (Klueh). Both theories are supported by evidence, but it is not yet understood which mechanism is dominant in killing the target cell. What is well understood, is that the silver must be in ionized form to interact with cell bodies, and is not as effective in its oxidized form prior to cell contact (Lok). The release of the positive silver ions, described by the equations below (Xiu),

$$4Ag(0) + O_2 \rightarrow 2Ag_2O$$

$$2Ag_2O + 4H^+ \rightarrow 4Ag^+ + 2H_2O$$
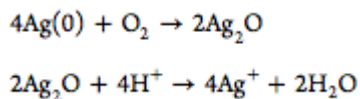
is proven to be toxic to bacteria because testing shows that antimicrobial activity is observed from the release of silver nanoparticles, and not from the control group of solid silver (Xiu). Silver in its nanoparticle form exhibits the greatest amount of antimicrobial activity, because of its ability to penetrate the cell wall. This precludes the option of using an ionically doped film with a compound such as silver nitrate in lieu of nanoparticles (Lok). The nanoparticles allow for a maximized effective surface area, because dispersing the same amount of silver into smaller particles will allow for more particles of smaller size, and therefore, the better the dispersion. This supports the nanoparticle approach used in industry and research for silver-based bacterial management.

3.2.3 SIZE AND DISPERSION OF THE SILVER NANOPARTICLES
Upon the addition of silver nitrate to the chitosan mixture, the silver ions chelate with the amino groups in the chitosan matrix prior to nanoparticle formation, ensuring an evenly dispersed initial spacing (Wei). In addition to dispersing the silver, these coordination sites play a vital role in the earlier discussed sequence of reactions that reduces the silver (Wei 2).

Previous literature, details an optimal set of conditions for small and well-dispersed nanoparticles, including synthesis, temperature, initial salt concentration, and solution pH (Wei). Wei imaged the resulting solutions with Transmission Electron Microscopy (TEM), to measure the size of the nanoparticles and to see how well they were dispersed throughout the solution (Figure 2). The resulting nanoparticles were found to be well distributed throughout the solution, and the size of them were somewhere between ten and thirty nanometers (Wei).
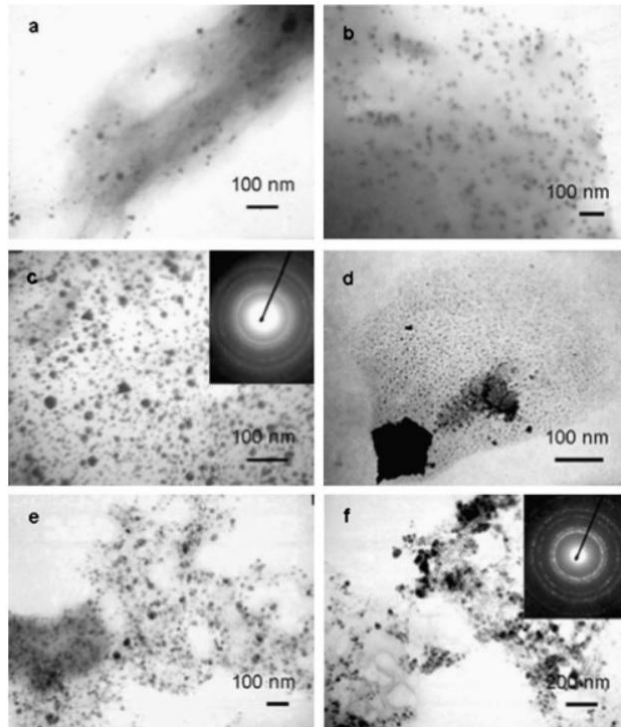
Figure 2: TEM images of metal NPs–chitosan bioconjugates by exposure of 30 mg of chitosan flakes to (a) 1.0 mM HAuCl4 at 95 C, (b) 6.0 mM AgNO3 at 95 C, (c) 1.0 mM HAuCl4 at 80 C, (d) 12.0 mM AgNO3 at 80 C, (e) 6.0 mM AgNO3 at 45 C, and (f) 6.0 mM AgNO3 at 45 C. Therein, (a–d) pH 5.9, (e) pH 7.0, and (f) pH 9.0. (Wei et al).

3.3 FILM PROPERTIES

3.3.1 CHITOSAN FILM ARRANGEMENT

Chitosan is a ring-structured polymer with a single ring being the monomer. The rings are attached by an oxygen functional group, and for our purposes, the silver nanoparticles chemically attach locally to the ammonia functional group by replacing hydrogen (Figure 3).
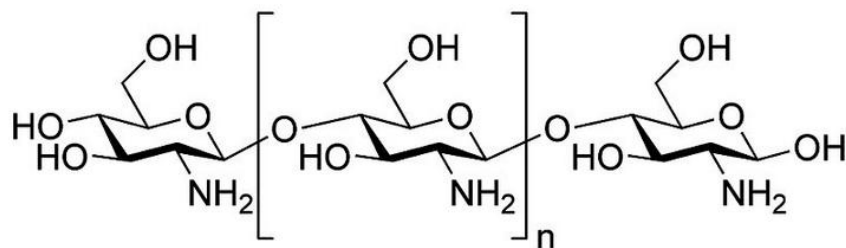

Figure 3: Chitosan ring structure and repeat unit bonding.

The chitosan reaches a certain saturation point (dependent on concentration of acetic acid used) in the film solution. When the film is in solution or even deposited onto a substrate, chitosan distributes itself evenly due to London Dispersion forces, Van der Waals forces, and a certain amount of steric interactions that repel and inhibit agglomeration.

3.3.2 MECHANICAL INTERACTIONS AND BONDING

Chitosan polymerizes into long chains and is a fairly dense polymer due to its ring structure containing both carbon and oxygen atoms. These chains are able to crosslink, and the chains bond to one another through hydrogen bonding on the hydroxyl functional groups, the lone carbon groups in the ring, and the ammonia hydrogens.

3.3.3 NANOPARTICLE DISTRIBUTION

While the nanoparticles are initially be well dispersed from the synthesis process, we cannot eliminate the settling of nanoparticles within the film as it cures. As previously discussed, the silver must ionize in order to have antimicrobial effect. The ubiquitous presence of water in the atmosphere and in the local environment around live cellular organisms provides an environment through which silver ions may diffuse (Klueh). This effectively means the nanoparticles will be able to act as an effective source of silver ions without direct contact with cellular bodies. We have decided to add polyethylene glycol (PEG) to our solution to increase the water retention and permeability of the polymer matrix, ensuring an adequate environment for silver ion diffusion. As a plasticizer, PEG will also alleviate the brittleness levan confers to the film.

3.3.4 THE NANOCOMPOSITE ANTIBACTERIAL EFFICACY

The main goal of this design is to make an antibacterial film. By determining the efficacy of the particles and the matrix in killing bacteria, we could derive an optimal composite with the greatest probability of killing bacteria. To do so we need to look at the rate at which bacterium is killed by the nanoparticles alone and the matrix alone. By applying the equation

$$\text{Population Growth Rate (t)} = [R_{growth}(t) - R_{kill}(t)]$$

where *R(t)* are the rate at which bacterial colonies grow and die. The rate at which the bacterium grows can be found in the literature while the *Population Growth Rate* can be experimentally measured. We then solve for the rate of killing for each component and determine what mixture would maximize the efficacy of our composite.

However, more important than the rate of bacterial killing, is the overall antibacterial property of the film. We used a K12-MC1655 strain of *e. coli* to test our samples according to the ASTM E2180-07 standard. The antibacterial properties of the film is determined by growing bacterial cells on the film and a control, to determine the colony forming units (CFU) per milliliter of film solution.

3.3.5 FILM DRYING

Drying is a mass transfer process, where a volatile solvent is removed by evaporation, leaving the solute material on a surface. Factors such as airflow, temperature and relative humidity can affect the drying rate. In a moving air-drying situation, which would be the most typical in this design, the drying rate is given by

$$\frac{dl_{s1}}{dt} = \frac{k_{g,v} M_w}{\rho_w RT} (p_v^*(T_F) - P_{VB})$$

where, dl_{s1}/dt is the change in the thickness of the film with time, $k_{g,v}$ is the mass transfer coefficient, with units of m/s, M_w is the molar weight of the solvent, ρ_W is the density of the solvent, R is the gas constant, T is the temperature, p_V^* is the saturated solvent vapor pressure, T_F is the temperature of the film and P_{VB} is the vapor pressure of bulk air (Kiil).

When it came time to design the prototypes and make the films we took the synthesized solutions and spread them out uniformly on a petri dish and gave them eight hours to dry. We initially kept the dishes covered to protect them from any debris that may have been floating around in the fume hood. However, we discovered that the films did not dry when they were covered. This led us to believe that the drying process needs to have an open-air source. The solvent does have a low vapor point that allows it to evaporate at room temperature, but it needs somewhere to evaporate to. This meant that we covered the top of the dish with a cloth, which allowed the solvent to evaporate while avoiding any contamination that could occur from debris.

3.3.6 FILM ADHESION

Adhesion is largely composed of 3 types of forces: mechanical, chemical and dispersive. Mechanical adhesion is due to physical entanglement and interlocking between two or more surfaces. One example is the adhesive effect of Velcro. In this case, the polymeric film would fill in vacancies or other defects on the aluminum oxide surface. While this is a considerable force for adhesion, it is not simple to model. A good way to visualize this adhesion is to look at the surface structures of our substrate, and to look at the relative sizes of our chitosan molecules to see if they will form a Velcro like mechanical fit.
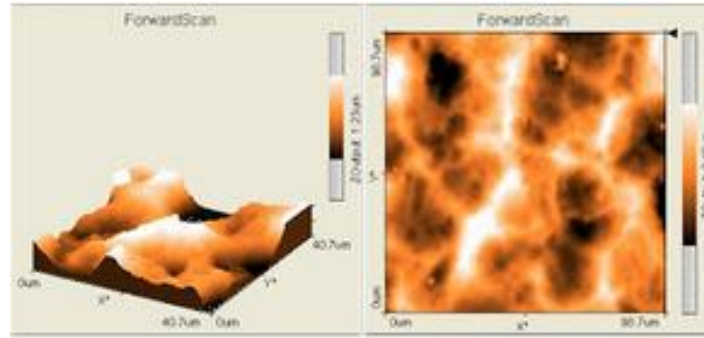
Figure 4: Atomic Force Microscopy 3D and 2D images of cell phone aluminum back substrate for anticipated film application surface.

Figure 4 is Atomic Force Microscopy (AFM) imaging of the back cover of an iPhone, which is made of aluminum. The surface is fairly rough, with peak and trough average differential height of approximately 1.5 μm (average of multiple scans, taken from bottom of troughs to top of peaks in several places). The nanoparticles are just that - nano, so they will fit in and physically adhere with no problem, but the greatest contribution to mechanical adhesion should come from the chitosan matrix. Chitosan solution is made from many chitosan molecules, which when hydrated in acetic acid, form a viscous solution with the average molecule smaller than one micron, so upon drying the chitosan will settle into the surface features and create a physical adhesion interaction.

Dispersive forces are also a factor in adhesion. Dispersive forces typically refer to van der Waals forces. For two flat surfaces, the work and force of van der Waals forces are

$$W = \frac{A}{12\pi D^2}$$

$$F = \frac{A}{6\pi D^3}$$

Where D is the distance between the two surfaces and A, the Hamaker constant, is given by

$$A = \pi^2 C \rho_1 \rho_2$$

where C is the coefficient of particle-particle pair interaction and ρ_1 and ρ_2 are the densities of the two materials. This relationship helps us understand that increased densities of the two materials help increase van der Waals forces. C is also known as the interaction constant, and thus cannot be derived

simply from known material properties. The Hamaker constant, however, may be approximated according to the Lifshitz theory of van der Waals interactions in terms of the McLachlan equation for interaction of two molecules, denoted by subscripts 1 and 2, and the medium, denoted by subscript 3.

$$A \simeq \frac{3}{4}kT(\frac{\varepsilon_1 - \varepsilon_3}{\varepsilon_1 + \varepsilon_3})(\frac{\varepsilon_2 - \varepsilon_3}{\varepsilon_2 + \varepsilon_3}) + \frac{3hv_e}{8\sqrt{2}} \frac{(n_1^2 - n_3^2)(n_2^2 - n_3^2)}{\sqrt{(n_1^2 + n_3^2)}\sqrt{(n_2^2 - n_3^2)}\{\sqrt{(n_1^2 + n_3^2)} + \sqrt{(n_2^2 - n_3^2)}\}}$$

where ε is the dielectric constant and *n* is the refraction index of the material and v_e is the orbiting frequency of an electron. While this is proven way for estimating the Hamaker constant, it is not within the realm of our possibilities to analyze the dielectric constant and refractive index of our film, as it has a very unique composition not thoroughly studied. Additionally, as the typical values of the Hamaker constant range from 10^{-19}J to 10^{-20}J our design assumes that the van der Waals forces for adhesion are negligible.

Although friction is not an adhesive force, we believe that the friction interaction between the film and the substrate can enhance the mechanical stability of the film on the substrate. Friction is simple defined by

$$F = \mu N sin(\theta)$$

where F is the force of friction, μ is the coefficient of friction and N account for normal, van der Waals and dispersive forces, as a result of the weight of the film. Understanding the forces of friction on the film will help us understand whether or not the film will move or delaminate when it is in use and serve as a means by which to further research mechanical adhesion.

Our decision to include levan in the polysaccharide mixture is based on its reported adhesive properties likely due to the density of entangling branches with hydroxyl groups (Costa). However, we are limited to the insight provided by literature on this material.

3.4 PROTOTYPING

3.4.1 PROTOTYPING IN THE LABORATORY
The aim of creating a prototype is to answer as many questions as possible, while minimizing the amount of questions a prototype can create. Parts of the project, that range from how well the antibacterial properties of the film work, to how well the film adheres to a surface, to the viscosity of the solutions, require prototypes to be built to fully figure out how these parts of the project will work.

Our initial prototyping was focused on the solution rheology. Because we did not expect the nanoparticles to have a considerable impact on the viscous properties, we aimed to establish proof-of-concept that the highest viscosity we could develop (further elucidated in section 4.2) could be sprayed with a commercial spray bottle that did not require additional pressurizing or specialized mechanism.

Multiple sets of solutions with different concentrations of nanoparticles were initially developed, with subsequent prototypes containing nanoparticles synthesized at varying temperatures. The aim of these prototypes was to analyze viscosity, film drying, adhesion and antibacterial properties. Prototyping occurred in both the nanoparticle fabrication laboratory, run by Dr. Cummings, and antibacterial testing laboratory, run by Dr. Sintim. The data we acquired from our prototypes allow us to interpolate certain trends on a general scale, but fail to show us the deeper intricacies of our design. Better validation of the design via prototyping was limited, mostly due to the restrictions to laboratory access and experimental abilities we had within such a short time.

The general process of prototyping starts with the solution synthesis, solution analysis, film development and finally, antibacterial analysis. Because each round of bacterial growth testing requires one week, it is the slowest step in the prototyping analysis, although it is one of the most crucial procedures. Unfortunately, because antibacterial films are tested by placing a film into broth to allow bacteria cells to grow, our prototype cannot be fully tested on the product. However, the final prototype will be designed based on the best data we acquired.

3.4.2 SIMULATIONS
We have decided to run two types of simulations where we would model molecular and fluid dynamics. A description of each follows below.

Molecular dynamics
The molecular dynamics simulation was placed on hold in favor of developing empirical data and equations. However, when it was actively being carried out, it was primarily carried out by the program Large-scale Atomic/Molecular Massively Parallel Simulator, or LAMMPS. LAMMPS is a classical molecular dynamics code that is run in DOS, and outputs realistic and accurate results. The problem with LAMMPS is that it can be difficult to program with without extensive practice and it does not present a visually appealing output. In order to develop more visually appealing results we planned to use Avogadro to create the molecules that will interact with each other. Avogadro is an advanced molecule editor and visualizer designed for use in computational chemistry, and molecular modeling. Avogadro is a more traditional CAD program that allows us to design the molecules for Chitosan and Levan graphically. This

design can then be formatted and inputted into LAMMPS so that we do not have to attempt to code it manually. This removes one of the potentials for user error during the coding process. It also gives a more visual representation that we would not get from the lines of code generated from a DOS prompt.

The visual outputs can be created with Visual Molecular Dynamics, or VMD. VMD is a program that takes LAMMPS code and displays, animates, and analyzes large biomolecular systems using 3-D graphics and built-in scripting. The combination of both VMD and LAMMPS gives us a visual representation of the interactions and flow that the molecules and nanoparticles would have with each other throughout the progression of the product.

As we have progressed with the programs, we have encountered several issues, especially with LAMMPS. There have been several difficulties that have been handled during both the installation, and the usage of the program. The installation of LAMMPS was extremely difficult. The installation required every single program that branched the interface between LAMMPS and the computer to be updated to the most recent version. Some of these updates had compatibility issues, and it took several hours to get the programs installed just so that LAMMPS was compatible with one of our laptops. From there the installation got even more complicated. There were two different installation packages, with very little data stating which package was the right one to use. There was also additional DOS work that needed to be carried out after the installation was complete. Once it was all done, the only way to tell it was complete was to use a sample file through DOS. If it didn't work, we had to go back to square one. The difficulties did not end with the installation. LAMMPS is a very computer science-centered program. It is built through, and runs with, coding that all comes from DOS. This means that one small error in the writing of, or execution, the program results in the simulation either failing or being inaccurate. The only way to effectively tackle this issue is through trial and error, which is a luxury we aren't afforded.

Fluid Dynamics
The goal of the fluid dynamics simulation is to create a model of the spray, where the model helps us in deriving the properties that allows the sprayability of the composite film. Although progress has been made in this front, we decided to shift our focus to the study of the interactions between the components of the composite during synthesis. A brief description of the work accomplish in fluid dynamics simulations.

To create a fluid dynamics model in ANSYS Fluent, we first needed to understand the mechanisms of the sprayer. This was accomplished by studying the sprayer that we purchased and creating a CAD model of the spray bottle (Figure 5a). The CAD drawings were made using the Creo Parametric software, which is

available through the university. The CAD model of the sprayer (Figure 5b), reviews the dimensions of the tubes through which the fluid flows and the dimensions of the piston casing, where fluid is drawn in and pumped out of the sprayer. These internal dimensions are important because they are the only relevant volumes of the sprayer when creating a fluid dynamics model in ANSYS fluent. By using only the relevant volumes, we can achieve the same results with a much lighter mesh than that using the entire sprayer casing, allowing faster modeling and eliminating concerns of software node limits, as demonstrated in a tutorial we used to learn fluid dynamics modeling with ANSYS (Figure 5c).
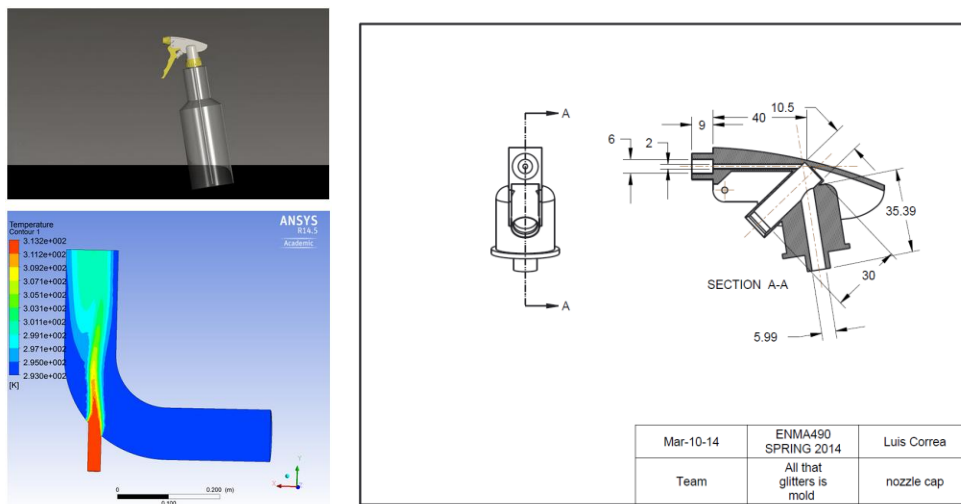

Figure 5a. top left: Creo Parametric rendering of spray bottle. **Figure 5b**. right: Technical drawing of the spray bottle head, which reviews the internal volumes needed for modeling on ANSYS. **Figure 5c.** bottom left:ANSYS model example.

4. EMPIRICAL DATA AND RESULTS

Here we report the results obtained while building and testing the prototype films. All of the data was collected from solutions and films that were applied to petri dishes, since we were on the early stages of prototyping. The goal was to validate our design before we could move towards the actual application we selected, the Apple iPhone 5.

4.1 FABRICATION OF CHITOSAN SOLUTION

Our first film samples were synthesized in Dr. Cumming's laboratory under graduate student supervision. To examine different viscosities, we began to make dilute acetic acid solutions containing 4,

6, 8, and 10 mg/mL of chitosan and 1 mg/mL of levan. We made 0.5 M and 1 % vol. acetic acid solutions based on different conventions used in literature. Due to the small quantities of solution prepared, it was logistically difficult to measure out small quantities of chitosan and levan with great precision, so only 8 and 10 mg/mL solutions of chitosan were made.

One of the aspects of the design we wanted to manipulate was the size of the nanoparticles. Our goal was to make them as small as possible, to allow for a higher amount of nanoparticles, which results in a higher overall surface area. The main ways we attempted to control the size of the nanoparticles was by manipulating the temperature, concentration of silver nitrate, and by changing the percentage of chitosan to PEG. We determined that the low percentages of PEG we added had no effect on the resulting solution. Changing the temperature and salt concentration, however, had a larger effect on the size of the nanoparticles. The two concentrations we used were 26 and 52 mM concentrations of silver nitrate. These were the standards that were set earlier by groups like the one led by Dongwei Wei, so we chose to follow them for the sake of design, time, and money. The 52 mM solutions created a smaller amount of nanoparticles with a higher average size, which was the opposite of our design goals, and was limited in terms of the amount of solutions made. We still used some of it to test for its antibacterial properties, but it was mostly used as a control. The initial 26 mM solution at eighty degrees celsius gave us a smaller nanoparticle size compared to its 52 mM counterpart. With this knowledge, we mainly used this concentration with regards to manipulating its temperature to see if any significant changes in nanoparticle size occurred.

The changes in nanoparticle size were determined by the usage of Dynamic Light Scattering, or DLS. The theory behind DLS is that when light hits small particles that it scatters in multiple directions. This is a phenomenon called Rayleigh scattering, and occurs when the particles are compared to the scattering wavelength. The particles are constantly moving in the solution due to Brownian Motion. This motion results in the distance between the particles and scattered light in the solution is changing with time. The scattered light then undergoes interference from the surrounding particles, which can be either constructive or destructive. This interference gives an intensity fluctuation, which can be manipulated to give the average size of the nanoparticles that are contained in the solution. There were several different solutions that underwent DLS testing to give us the size of the nanoparticles. These different sample sets can be seen below in Table 1 and Figure 6, with the chart comparing temperature to nanoparticle size for four of the 26 mM samples.

Table I:

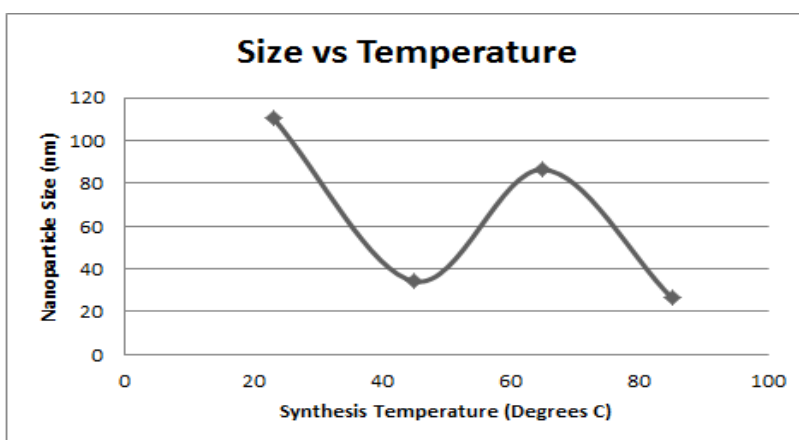| Date	Molarity	Sample #	Calculated mass AgNO3 (g)	Experimental mass AgNO3 (g)	Temperature (°C)	Size data (nm)
5-May	26	1	0.0883	0.0877	45	34.23
		2	0.0883	0.0875	45	45.20 (42.1% vol), 5074 (57.9% vol)
1-May	26	1	0.0883	0.0901	65	86.45
		2	0.0883	0.0912	65	74.61 (48.8% vol), 5011 (51.2% vol)
28-Apr	26	1	0.0883	0.0912	85	26.33
		3	0.0883	0.0879	Room Temperature	110.6
	52	1	0.1766	0.1762	85	40.74 (56.3% vol), 4775 (42.7% vol)

Figure 6: an analysis of the average size of nanoparticles based on synthesis temperature

The resulting chart and graph could show that the particle size does decrease as the synthesis temperature increases. While this is not a linear relationship, this could simply be due to there not being enough iterations of each sample to see if certain results are outliers. While we wanted to push the temperature past 85, we were restricted by time, and worried about a higher temperature breaking down with our polysaccharide, and leaving us with a solution that would not be able to form.

The solutions turned an orange color when they were finished. Silver nanoparticles are orange, with everything else in the solution, including the dissolved salt and chitosan, being clear. This gave us an indicator that the synthesis had taken place and that we had silver nanoparticles contained within. However, one unintentional error left us with brown solutions. One set of samples was left next to a window over the course of a weekend, and it ended up breaking down. We believe that this means the samples are UV sensitive. This theory has been reinforced by the fact that none of our samples that have been left in an enclosed environment underwent these changes. Figure 7 below shows a set of "good" samples, followed by one that was broken down by UV rays.

Figure 7: The orange vials are those with synthesized silver nanoparticles suspended in chitosan/acetic acid solution. The brown vials were likely damaged by UV exposure during a weekend by a window.

4.2 VISCOSITY OF CHITOSAN IN ACETIC ACID

The viscosity of the solutions are comparable with those of olive oil and maple syrup and will not compromise sprayability of the solution. Table I reports the viscosity of samples containing 10 mg of chitosan and either 26 or 52 mM $AgNO_3$ dissolved in 20 ml of 1% vol. acetic acid.

Table II: Viscosity measurements

Sample ID	Measurement 1 [cP]	Measurement 2 [cP]	Measurement 3 [cP]
1% vol. CH_3COOH 10 mg chitosan	164.5	162.8	163
26 mM $AgNO_3$ at 85°C stirred	124.3	123.8	123.7
52 mM $AgNO_3$ at 85°C stirred	120	119.1	119.6
26 mM $AgNO_3$ at 85°C not stirred	155.5	154	154.2
52 mM $AgNO_3$ at 85°C not stirred	158.8	161.2	159.2
26 mM $AgNO_3$ at 25°C not stirred	174.6	175	174.7
52 mM $AgNO_3$ at 25°C not stirred	158.5	158.2	157.7

The conditions during the synthesis of the nanoparticles are main distinctions between the six samples. Two of the samples were synthesized at 85°C with a magnetic stirrer, two were synthesized 85°C without a magnetic stirrer and two were synthesized at room temperature, so they could be compared with a sample without nanoparticles. Figure 8 shows an attempt to relate the nanoparticle synthesis conditions to the viscosity. While we understand that more data is necessary to relate the nanoparticle synthesis conditions to the viscosity, data collection was limited by access to laboratories and the timeline of the project. Nevertheless, the early data, suggests that stirring the samples while synthesizing the nanoparticles, lowers the viscosity. We also found through DLS measurements of the nanoparticles size, that stirring lowers the size of the nanoparticles, 26 nm for 85°C stirred and 111 nm for 85°C not stirred. This suggests that stirring the solution during nanoparticle growth leads to smaller nanoparticles, which is ideal, and lowers the average molecular weight of the polymer chains, lowering the viscosity. While ideally the viscosity needs to be around 180 cP, the drop of about 60 cP in viscosity does not greatly compromise our design.
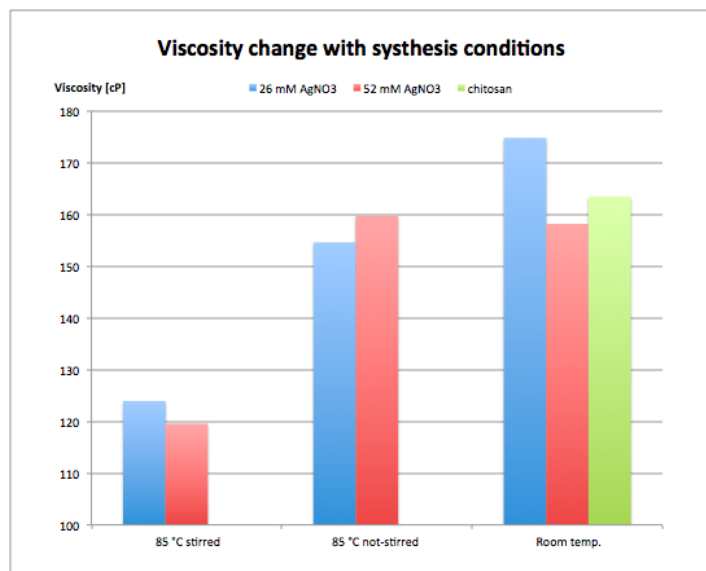
Figure 8: *An attempt to relate the nanoparticle synthesis conditions and the viscosity of six samples was made. Two of the samples were kept at room temperature, so that their viscosity could be compared to that of the solution without nanoparticles. Unfortunately,, time and access to laboratory, limited the number of measurements available for analysis.*

4.3 FILM DRYING

Our design goal for drying time is 8 hours, but our experiments suggest that actual drying time may be faster. Experiments where we tested the film against various surfaces show that the film dries within less than 3 hours at room temperature in an open space. During the viscosity measurements, we tested the film against a utility knife, Mylar sheet, a laboratory Corian workbench and a glass beaker. We found that the film dried between 90 minutes and 3 hours. The variation is likely due to film thickness and the material on which the film was deposited. The film was not sprayed, instead, a droplet was deposited on the surface and either allowed to dry, or was spread with a wooden dowel. Although these experiments were not well controlled, they reviewed interactions between the film and other materials, helping the group narrow down the target material surface in our design. One such example is the case of the utility knife.
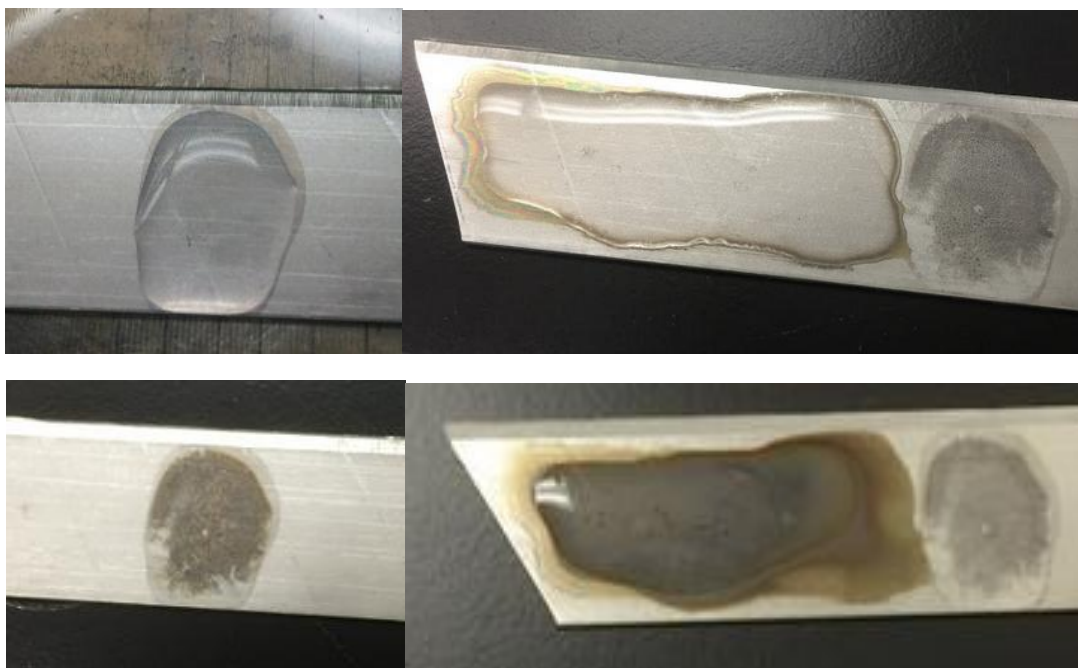
*F*igure 9: *The effects of acetic acid on tool steel. Starting on top left moving clockwise; a.) chitosan/acetic acid composite drying on tool steel at elevated temperature, on hot plate, before reaction took place b.) The same composite drying at room temperature before reaction took place, the stains left from a) are also visible. c) and d) The stains left on the tool steel are obvious during and after drying.*

Our observation of the effects of the film on the surface of the tool steel, which is used to make utility knifes, led us to research what could have caused the following effects. When we deposited the film on the tool steel, we observed corrosion in the interface between the substrate and the solution, which left permanent damage on the material's surface (Figure 9c and 9d). We learned that acetic acid is a well known corrosive agent in mild steel (Tran). Acetic acid undergoes reduction at the surface of the metal,

$$2HAc + 2e^- \rightleftharpoons H_{2\,(g)} + 2Ac^-_{(aq)} \qquad and \qquad 2H^+_{(aq)} + 2e^- \rightleftharpoons H_{2\,(g)}$$

which is the reduction of hydrogen ions typical in acids. An anodic reaction,

$$Fe_{(s)} \rightleftharpoons Fe^{2+}_{(aq)} + 2e^-$$
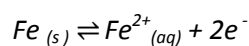
occurs simultaneously at the surface of the metal, which balances the charges and leads to the dissolution of iron, therefore, steel should be avoided. While the acetic acid corrosion of steel is a well-documented phenomenon, it is also well known that aluminum does not corrode in contact with acetic acid. This is because the Al_2O_3 layer serves as a passivation layer, which prevents the dissolution of aluminum in the presence of acetic acid at low temperature (Davis), where the film is designed to

operate.

4.4 FILM THICKNESS

We measured the thickness of the films by measuring 10 random regions of the film and finding the average thickness throughout the film. It ranges around 60 and 70 μm, which is only about 10-20 μm above the thickness given by our design.

Table III: Thickness of chitosan-nanosilver films

Sample ID	26 mM #1 65 C	26 mM #2 65 C	26 mM #1 45 C	26 mM #2 45 C
Thickness (μm)	110	70	20	20
Thickness (μm)	30	70	20	30
Thickness (μm)	50	100	30	30
Thickness (μm)	50	80	40	40
Thickness (μm)	70	70	30	40
Thickness (μm)	110	50	70	70
Thickness (μm)	130	50	110	110
Thickness (μm)	40	40	120	130
Thickness (μm)	50	40	90	110
Thickness (μm)	70	60	80	130
Average (μm)	**71**	**63**	**61**	**71**

4.5 ANTIBACTERIAL TESTING

Testing how the films behave and react to the introduction of harmful bacteria is essential to our project goals. To do so, we got permission to use a bacteria-testing facility in the biochemistry building in the Sintim research group. We tested our film's antibacterial properties against a strain of non-enterogenic, Escherichia coli (*e. coli*). E. coli. are used frequently as a benchmark organism for antibiotic testing. E. coli is a prokaryotic bacteria, and has a cell membrane and wall identical to other prokaryotic bacteria, so its reaction to our nanoparticles and chitosan will be uniform with other types of similar bacteria. It is important to be able to remove these bacteria that can be transferred by touch from surfaces we touch

frequently, such as our cell phones.

The process started with a rinsing of our glassware with soap and distilled water, autoclaving the materials to kill any and all bacteria, so we have a sterile testing environment. With 0.8 g NaCl, 0.3 g agar (a polysaccharide derived from algae), and 100 mL of distilled water, we made a solution to be the solid substrate in petri dishes to grow bacterial cultures. Next, we cleaned the fume hood with ethanol and lit a Bunsen burner to deplete oxygen from the incoming air. We cut our previously prepared films into 3x3 cm squares. One test cycle had two squares of each chitosan film, 26 and 52 mM AgNO$_3$ synthesized nanoparticles - chitosan film and a pair of chitosan film without AgNP, so six tests in total. One square specimen of each was taken as a zero hour control test, and the other of each served as a 24 hour incubation in a incubator.

We then introduce the E. coli. We diluted the stock grown E. coli solution down with a beef broth to make a comparable number of culture forming bacteria cells. We added 100 µL of bacterial solution into 50 mL of broth, and coated the films, leaving the 24 hour samples to incubate and transferring the zero hour films into 50 mL broth vials to mix in a sonicator and vortex mixer. From there, we diluted the broth from each film into three dilutions, and spread these dilutions onto agar substrates in petri dishes to be incubated and grow cultures.
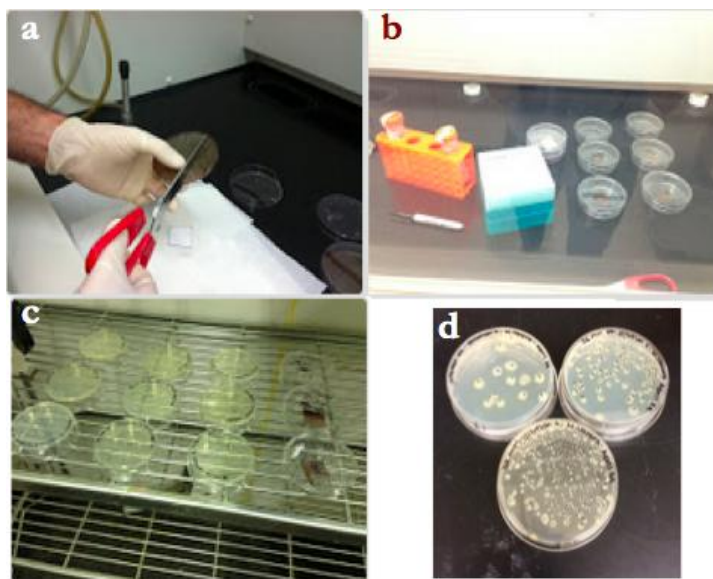

Figure 10: (a) the films into squares, (b) applying the bacterial broth to film,(c) bacterial dilutions and films incubating, (d) grown cultures ready to be counted

The cultures are then counted (if any are grown) and documented. Table IV, the culture counts are

shown for two testing cycles. Samples from the later dates did not grow any cultures and were omitted.

Table IV: Bacteria culture counts

Date	Molarity AgNO3	Dilusion #	Culture count	Hour
5/8/2014	52 mM	3	4	0H
5/1/2014	chitosan	1	17	0H
5/1/2014	26 mM	1	94	0H
5/1/2014	52 mM	1	342	0H
5/1/2014	chitosan	2	0	0H
5/1/2014	26 mM	2	0	0H
5/1/2014	52 mM	2	0	0H
5/1/2014	chitosan	3	0	0H
5/1/2014	26 mM	3	0	0H
5/1/2014	52 mM	3	2	0H
Date	Molarity AgNO3	Dilusion #	Culture count	Hour
5/9/2014	52 mM	3	4	24H
5/1/2014	chitosan	1	0	24H
5/1/2014	26 mM #1	1	4	24H
5/1/2014	26 mM #2	1	7	24H
5/1/2014	chitosan	2	0	24H
5/1/2014	26 mM #1	2	0	24H
5/1/2014	26 mM #2	2	0	24H
5/1/2014	chitosan	3	0	24H
5/1/2014	26 mM #1	3	0	24H
5/1/2014	26 mM #2	3	1	24H

In many cases, the bacteria was killed and not allowed to grow cultures. In other cases, few cultures were grown, and in other cases yet, many cultures were grown. The graduate student who supervised us, informed us that it is common to get data that is not characteristic of the trend. This can arise from messed up bacterial concentrations and contaminated substrates. We would need many more test runs to get conclusive data trends.   From this data, we can only say that the chitosan and chitosan/nanoparticle killed bacteria at these concentrations.

4.6 FILM ADHESION TO ALUMINUM VIA SPRAY APPLICATION

Multiple aspects of our film design indicate that our solution would be able to sprayed based on the viscosity of the solution. Additionally, the AFM analysis and initial design based on surface wetting both indicated that the film would be able to properly be sprayed as a film unto the iPhone surface.

Spray testing unto aluminum surfaces, both tin foil and the iPhone, showed poor potential for film development based on the formation of droplets and a lack of even coating. This can be seen in Figure 11(a) and Figure 11(b). Compared to Figure 11(c), which shows the solution distribution after multiple sprays unto a laboratory paper wipe, the poor wetting of the aluminum surfaces indicate that the surface energy of the liquid-gas and liquid-surface interfaces are very high.
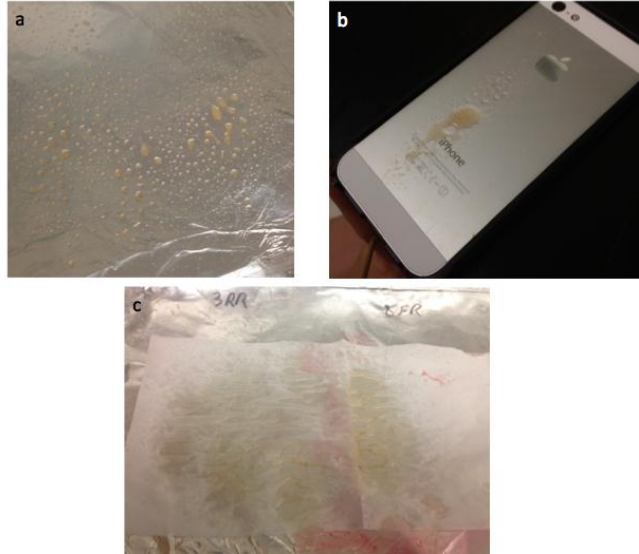
Figure 11: *Photographic representations of the spray dispersion and wetting*
(a) a dozen sprays unto aluminum foil (b) a single spray unto the iPhone surface
(c) a dozen sprays unto a wipe tissue

Because of this, the spray application may not be best as a one-step process to develop a film on the aluminum surface. Assistance from the user, such as spreading with a Q-Tip may be an approach to resolve poor wetting while still allowing for spray application.

5. FACILITIES

Glen L. Martin Hall Computer Lab

One of the facilities used for the preliminary part of the project was the computer lab in Glenn L Martin Hall. We used the computers there to access programs such as ANSYS, when working on computational modeling. The programs we considered using to model our project are LAMMPS, ANSYS Workbench, Avogadro, and VMD. LAMMPS, Avogadro, and VMD are used to model the molecules and nanopowders to determine their interactions and ANSYS Workbench is used to model the container that the solution will be held in and how it will be inserted into the environment from the container by the means of a spray nozzle.

Cummings Research Group

To synthesize the nanoparticles we worked in Dr. Cumming's lab in the Chemical Nuclear Engineering Building . His laboratory is equipped with the appropriate measuring and synthesis tools for our nanoparticle and chitosan solutions. Additionally, the laboratory had space where it was safe for us to

store our materials during the time we were conducting experiments.

Sintim Research Group

We used Dr. Sintim's cell culture laboratory to test the antibacterial properties of the film. This lab is within the chemistry department. Bacterial cultures and antibacterial testing were all conducted in this laboratory, in addition to the adjacent incubation chamber.We had ample help from his graduate student, Yue Zheng, throughout this entire process.

Maryland Energy Research Center (UMERC)

Additionally, the viscosity measurements were carried out at the University of Maryland Energy Research Center, or UMERC.

6. MILESTONES & DELIVERABLES

Our project encompasses four aspects: design, modeling, prototyping and testing. Design is the initial and most important milestone to complete as it dictates the future of the project. The modeling and prototyping phases can be done in parallel as experimental data can help render better models. Lastly, because the antibacterial nature of the nanosilver is not fully understood, it is difficult to accurately model this.

1. Set a Design Goal: This was the first initial milestone and predominantly required research on literature and an assessment of available resources. This step was intended to define the expected and desired properties and parameters of our product for optimal performance.
2. Determine Procedure for Desired Properties: This involves taking the design goals and attributing specific nanoparticle sizes and synthesis methods to them. This also involves setting a solution composition that will have a sprayable viscosity. Gaining insight on the formation of the nanoparticles and the likely geometric arrangement of the film in its dried state will be vital for predicting how to best optimize this arrangement.
3. Model Film Arrangement: This involved understanding the polymerization and arrangement of the chitosan and the arrangement and movement of the nanoparticles within the film. This will help model both antibacterial properties and adhesion.
4. Model Antibacterial Properties: This depends on the arrangement of the components of the composite film and the assumed theories of how they act in antibacterial manners. This will allow our design to reach desired antibacterial properties.

5. <u>Model Film Adhesion:</u> This involves determining the modes of adhesion of the film (mechanical, chemical or dispersive) and the film properties that affect adhesion in order to model it. This will determine adhesive properties, how they can be promoted and what will lead to film delamination. This modeling depends on the arrangement of the film.

6. <u>Experimental Data Gathering:</u> Due to the limitations in previous research and in the mathematical descriptions of various aspects of our design, we intended to experimentally gather some data in order to finalize our design. Most importantly, viscosity measurements of our various solutions can help with the design of a sprayable solution but also further model interactions between the polymer matrix and silver nanoparticles.

7. <u>Prototyping and Testing:</u> This is the final milestone we hope to accomplish within the scope of our semester, implementing our designs and testing the antibacterial properties, hopefully obtaining results that align with our design or can be explained phenomenologically.

7. CONCLUSION

Over the course of the semester, this team worked towards designing a sprayable antibacterial nanosilver composite film, to be applied to the aluminum oxide backside of the Apple iPhone 5. As stated at the beginning of this report, our design goals were to design an antibacterial film that would have an antibacterial efficacy of 5×10^5 CFU/ml, a 50 μm thickness, overnight drying, a sprayable application and adhesion to the aluminum oxide surface of the iPhone.

Our technical approach encompassed principles from our past four years as undergraduates in the Materials Science and Engineering department, and aimed to give us a complete understanding of our design. In many cases, the theories used in our design gave our group a logical and wholesome direction for our project. However, as is often the case, a sound design does not always translate to corroborating experimental data or working prototypes. We accomplished all of our milestones for this project. With our prototypes, we accomplished our goals with respect to antibacterial efficacy, drying time and adhesion. We believe that this makes for a promising design that needs future work with regards to experimental data and prototype. Overall, we are happy with what we accomplished for our senior design project and wish we could have had more time to continue our work.

8. Updated Work Plan
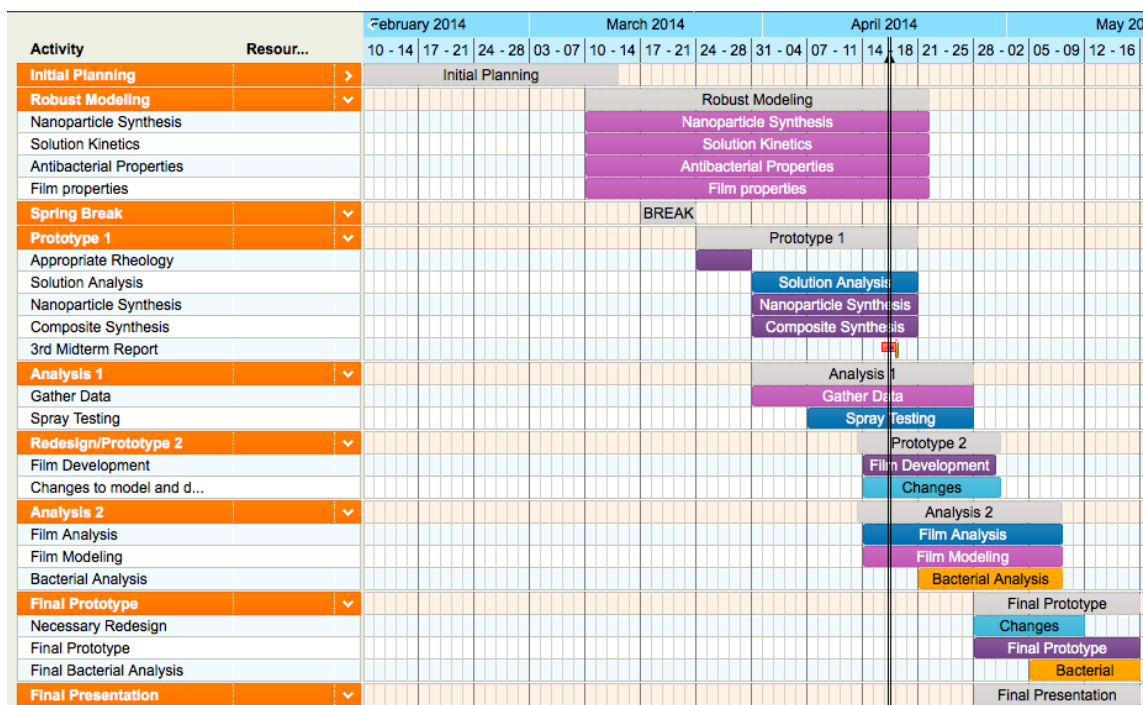
9. Updated Budget

Our budget remains unchanged since the last quarter.

Purchase	Cost
Pressure Sprayer	$4.97
Levan polysaccharide	$150.00
Chitosan polysaccharide	$65.12
Petri dishes	$20.98
Silver Nitrate	$62.46
Poster and Misc. Materials	$100
Remaining Budget	**$596.47**

10. TEAM ROLES

Mercedes Valero is team leader. She is a senior materials science and engineering student specializing in materials for energy. She has research experience with organic wet laboratory sample preparations and AFM analysis. Within the team, she is the leader and coordinator. She works primarily with sample design and analysis

Benjamin Lee is the treasurer. He is a senior materials science and engineering student specializing in biomaterials and soft materials, and has organic laboratory experience with preparing and isolating chemical components and solutions. He manages the project budget, and works with sample design and prototyping.

Matt Reilly is the secretary. He takes minutes at every team meeting, acts as a scribe in the lab setting, and updates the group section on the class website when necessary. He reads source articles and reports to the group. He is a senior materials science and engineering major with a specialization in materials for energy. He will be pursuing his MS/PhD in MSE after graduation. Matt has experience in project management, customer service, and ceramic powder processing into solid oxide fuel cells. He is familiar with laboratory procedure and testing. He will help with viscosity measurements, making the liquid into a sprayable film, lab synthesis, and bacterial testing.

Luis Correa is the facilities organizer and point of contact with external sources. He will be responsible for scheduling time at laboratories and characterization tools needed for the completion of the project. He is a senior in materials science and engineering specializing in materials for energy. His research experience involve the development and characterization of solid oxide fuel cells, from slurry preparation to testing, as well as, characterization of mechanical properties of thin films through nanoindentation. He has experience with organic chemistry laboratories and is comfortable working with chemical and bacteria. Within the team, he works with modeling, characterization and prototyping.

Nathan Cloeter is the Deputy Group Leader. He is a senior materials science and engineering student specializing in biomaterials. He has experience with designing and testing dental composite samples, as well as an extensive history with AutoCAD that spans several years. Within the team, he assists the team leader with her managerial responsibilities. He works primarily with sample design, CAD modeling, and prototyping.

WORKS CITED

ASTM E2180-07(2012), "Standard Test Method for Determining the Activity of Incorporated Antimicrobial Agent(s) In Polymeric or Hydrophobic Materials" Book of Standards, Vol 11.05

Brookfield. "Brookfield digital viscometer." *Brookfield engineering laboratories*. MIddleboro, MA: <http://www.brookfieldengineering.com/products/viscometers/laboratory-dv-e.asp>.

Costa, R., Neto, A., Calgeris, I., Correia, C., Pinho, A., Fonseca, J., Oner, E., Mano, J. "Adhesive nanostructured multilayered films using a bacterial exopolysaccharide for biomedical applications." *Journal of Materials Chemistry B* (2013) 1, 2367-2374

Davis, Joseph R.. *Corrosion of Aluminum and Aluminum Alloys*. Materials Park, OH: ASM International, 1999. Print.

Esawy, M. A., Ahmed, E. F., Helmy, W. A., Mansour, N. M., El-Senousy, W. M., El- Safty, M. M. "Antiviral levans from *Bacillus spp*. isolated from honey." *The Complex World of Polysaccharides* (2012) 195-214

Ferrer, M., Hickock, N., Eckmann, D., and Composto, R. "Antibacterial biomimetic hybrid films." *Soft Matter* 8 (2012) 2423-2431

Guo, L., Yuan, W., Lu, Z., Ming Li, C. "Polymer/nanosilver composite coatings for antibacterial applications." *Colloids and Surfaces A: Physicochemistry Engineering Aspects* 439 (2013) 69-83

Huang, Haizhen, and Xiurong Yang. "Synthesis of Polysaccharide-stabilized Gold and Silver Nanoparticles: A Green Method." *Carbohydrate Research* 339 (2004): 2627-631

Kiil S. "Drying of latex films and coatings: Reconsidering the fundamental mechanisms." *Progress in Organic Coatings*. 2006; 57 (3) : 236-250

Klueh, U., et al. "Efficacy of silver-coated fabric to prevent bacterial colonization and subsequent device-based biofilm formation." *Journal of Biomedical Material Research* 53 (6) (2000) 621-631

Lok, Chun-Nam, et al. "Silver nanoparticles: partial oxidation and antibacterial activities." *Journal of Biological Inorganic Chemistry* 12 (4) (2007) 47-534

Moritz, Michal, Gezke-Moritz, Malgorzata. "The newest achievements in synthesis, immobilization and practical applications of antibacterial nanoparticles." *Chemical Engineering Journal* 228 (2013) 596-613

Pierre, Alain C. , Introduction to Sol-Gel Processing, (1998), Kluwer, Norwell, MA

Reigel, Anna, et al. "Preparation and characterization of chitosan-silver nanocomposite films and their antibacterial activity against Staphylococcus aureus." *Nanotechnology,* 24 (2013)

Richardson, J.F. and Zaki, W.N., "Sedimentation and Fluidisation: Part I." *Institution of Chemical*

Engineers, 32 (1954)

Song, Sora. "Study: 1 in 6 Cell Phones Contaminated With Fecal Matter | TIME.com."*Time*. Time, n.d. Web. 25 Apr. 2014. <http://healthland.time.com/2011/10/17/study-1-in-6-cell-phones-contaminated-with-fecal-matter/>.

Srinivasa, P.C., Ramesh, M.N., Kumar, K.R., Tharanathan, R.N. "Properties of chitosan films prepared under different drying conditions." *Journal of Food Engineering*, 63 (2004) 79-85

Tran, Thu, et al. "Investigation of the Mechanism for Acetic Acid Corrosion of Mild Steel.". Houston, TX: 2013. 2487. Print.

Wei, Dongwei, et al. "The synthesis of chitosan-based silver nanoparticles and their antibacterial activity." *Carbohydrate Research*, 344 (2009) 2375-2382

Wei, Dongwei (2), et al. "Chitosan as an active support for assembly of metal nanoparticles and application of the resultant bioconjugates in catalysis." *Carbohydrate Research*, 345 (2010) 74-81

Xiu, Zong-Ming et al. "Negligible Particle-Specific Antibacterial Activity of Silver Nanoparticles" *Nano Letters,* 4271 (2012)